Accepted Manuscript

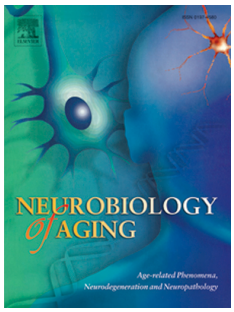

Cerebral changes and disrupted gray-matter cortical networks in asymptomatic older adults at risk for Alzheimer's disease

J.L. Cantero, M. Atienza, P. Sanchez-Juan, E. Rodriguez-Rodriguez, J.L. Vazquez-Higuera, A. Pozueta, A. Gonzalez-Suarez, E. Vilaplana, J. Pegueroles, V. Montat, R. Blesa, D. Alcolea, A. Lleo, J. Fortea

PII: S0197-4580(17)30405-0

DOI: 10.1016/j.neurobiolaging.2017.12.010

Reference: NBA 10106

To appear in: *Neurobiology of Aging*

Received Date: 23 March 2016

Revised Date: 26 November 2017

Accepted Date: 12 December 2017

Please cite this article as: Cantero, J., Atienza, M, Sanchez-Juan, P, Rodriguez-Rodriguez, E, Vazquez-Higuera, J., Pozueta, A, Gonzalez-Suarez, A, Vilaplana, E, Pegueroles, J, Montat, V, Blesa, R, Alcolea, D, Lleo, A, Fortea, J, Cerebral changes and disrupted gray-matter cortical networks in asymptomatic older adults at risk for Alzheimer's disease, *Neurobiology of Aging* (2018), doi: 10.1016/j.neurobiolaging.2017.12.010.

Cerebral changes and disrupted gray-matter cortical networks in asymptomatic older adults at risk for Alzheimer's disease

JL Cantero,[1,2*] M Atienza[1,2], P Sanchez-Juan[2,3], E Rodriguez-Rodriguez[2,3], JL Vazquez-Higuera[2,3], A Pozueta[2,3], A Gonzalez-Suarez[2,3], E Vilaplana[2,4], J Pegueroles[2,4], V Montat[2,4], R Blesa[2,4], D Alcolea[2,4], A Lleo[2,4], J Fortea[2,4]

[1]Laboratory of Functional Neuroscience, Pablo de Olavide University, Seville, Spain

[2]CIBERNED, Network Center for Biomedical Research in Neurodegenerative Diseases, Spain

[3]Service of Neurology, University Hospital "Marques de Valdecilla". University of Cantabria. IDIVAL, Santander, Spain

[4]Department of Neurology, Institut d'Investigacions Biomediques Sant Pau-Hospital Santa Creu i Sant Pau, Universitat Autonoma de Barcelona, Barcelona, Spain

*Corresponding author:

Jose L. Cantero, Ph.D.
Laboratory of Functional Neuroscience
Pablo de Olavide University
Ctra. de Utrera Km 1,
ES-41013 Seville, Spain

E-mail: jlcanlor@upo.es
Phone: +34 954 977433

Abstract

The diagnostic value of cerebrospinal fluid (CSF) biomarkers is well established in AD, but our current knowledge about how abnormal CSF levels affect cerebral integrity, at local and network level, is incomplete in asymptomatic older adults. Here, we have collected CSF samples and performed structural magnetic resonance imaging (MRI) scans in cognitively normal (CN) elderly as part of a cross-sectional multicenter study (SIGNAL project). To identify group differences in cortical thickness, white matter (WM) volume and properties of structural networks, participants were split into controls (N=20), positive amyloid-β ($A\beta_{1\text{-}42}^{+}$) (N=19), and positive phosphorylated tau ($p\text{-}tau^{+}$) (N=18). The $A\beta_{1\text{-}42}^{+}$ group exhibited thickening of middle temporal regions, while $p\text{-}tau^{+}$ individuals showed thinning in the superior parietal and orbitofrontal cortex. Subjects with abnormal CSF biomarkers further showed regional WM atrophy and more segregated cortical networks, the $A\beta_{1\text{-}42}^{+}$ group showing heightened isolation of cingulate and temporal cortices. Collectively, these findings highlight the relevance of combining structural brain imaging and connectomics for *in vivo* tracking of AD lesions in asymptomatic stages.

Keywords: Preclinical Alzheimer's disease, SNAP, CSF biomarkers, cortical thickness, structural cortical networks, white matter.

1. Introduction

Deposition of intracellular neurofibrillary tangles (NFT) and extracellular Aβ plaques, the main pathological features of AD, promote cerebral insults characterized, at macroscopic level, by regional atrophy of AD-related brain regions, and microscopically by cumulative neuronal loss, synaptic dysfunctions, and alterations of dendritic arborization (Bobinski et al., 2000). Accumulated evidence suggests that Aβ depositions and AD-like neurodegenerative changes are present in the brain of a high proportion of asymptomatic older individuals (Jack et al., 2014; Gordon et al., 2016), supporting interventions in CN at-risk subjects aimed to postpone, reduce the risk of, or prevent the clinical onset of AD (Reiman et al., 2010).

Cerebrospinal fluid (CSF) is in direct contact with the brain and therefore its composition reveals biochemical changes occurring in the extracellular spaces. Accordingly, CSF concentrations of $A\beta_{1-42}$, total tau (t-tau), and p-tau indirectly reflect the presence of Aβ plaques, axonal damage, and accumulation of NFT, respectively (Blennow and Hampel, 2003; Hampel et al., 2010). The validity of these CSF biomarkers has been further confirmed in brain autopsy of AD patients, showing that the lower the $A\beta_{1-42}$ levels, the higher the density of amyloid plaques (Strozyk et al., 2003), and the higher the concentration of p-tau, the larger the NFT burden (Buerger et al., 2006; Tapiola et al., 2009). Previous studies have established the presence of AD lesions to a lesser degree in CN elderly subjects at the time of death (Knopman et al., 2003; Dugger et al., 2014), suggesting that AD pathology precedes clinical symptoms. In line with these findings, the presence of abnormal concentrations of $A\beta_{1-42}$ and p-tau in CSF of CN elderly has been associated with poorer cognitive performance (Hedden et al., 2013; Pettigrew et al., 2015), increased risk of developing cognitive decline (Fagan et al., 2007; Roe et al., 2013), and structural and functional changes in the

cortical mantle (Sheline et al., 2010; Fortea et al., 2010; 2011; Bateman et al., 2012; Mattsson et al., 2015).

Measurements of cortical thickness have gained importance in AD research since they provide a powerful non-invasive and *in vivo* estimate of neuronal shrinkage and neuronal loss in humans (Fischl and Dale, 2000; Salat et al., 2004). **Whereas most of the studies performed to date have shown gray matter (GM) reductions in asymptomatic older adults with cerebral amyloidosis (e.g., Storandt et al., 2009; Fjell et al., 2010; Tosun et al., 2010; Becker et al., 2011; Arenaza-Urquijo et al., 2013; Doherty et al., 2015), others have found increased gray matter associated with abnormal $A\beta_{1-42}$ concentrations (Chetelat et al., 2010; Fortea et al., 2010; 2011; 2014; Johnson et al., 2014), raising the question of whether cortical hypertrophy in $A\beta_{1-42}^{+}$ asymptomatic elderly subjects should also be considered as a signature of preclinical AD.** However, no study to date has evaluated the independent effect of cerebral amyloidosis and neurodegeneration on cortical thickness and cerebral WM volume as revealed by abnormal CSF levels of $A\beta_{1-42}$ and p-tau respectively.

Variations in GM covariance networks have shown to be helpful at discriminating among CN elderly subjects, prodromal and clinical AD stages (He et al., 2008; Yao et al., 2010; Spreng and Turner, 2013; Tijms et al., 2013; Romero-Garcia et al., 2016). Most of these studies have revealed that GM networks of MCI/AD patients have a less optimal topological organization characterized by increased segregation and decreased integration (He et al., 2008; Tijms et al., 2013; Romero-Garcia et al., 2016). But whether topology of GM networks is similarly affected in CN subjects with abnormal CSF $A\beta_{1-42}$ or p-tau levels is unknown.

To our knowledge, only one study has previously assessed the relationship between CSF $A\beta_{1-42}$ levels and GM network disruptions in CN adults (Tijms et al., 2016). Results showed that lower $A\beta_{1-42}$ levels were linearly associated with lower connectivity density, and nonlinearly with lower clustering values and higher path length values, which is indicative of a less efficient network organization (Tijms et al., 2016). Nevertheless, the potential contribution of abnormal p-tau levels on topological properties of GM networks was not specifically assessed in that study. Furthermore, 18% of their participants showed a Clinical Dementia Rating (CDR) score of 0.5 and only 13% of them had abnormal $A\beta_{1-42}$ levels (i.e., < 550 pg/mL), remaining uncertain whether $A\beta_{1-42}$-related changes in topological organization of GM networks could indeed be extrapolated to preclinical AD stage 1.

In the present study, we have compared patterns of cortical thickness and cerebral WM between CN elderly subjects showing normal and pathological CSF levels of either $A\beta_{1-42}$ or p-tau. We hypothesize that individuals with pathological CSF $A\beta_{1-42}$ levels will show thickening of AD-related cortical regions likely due to neuronal hypertrophy and/or Aβ-associated neuroinflammation, whereas those with pathological CSF p-tau levels will exhibit patterns of cortical thinning in vulnerable AD regions probably caused by NFT-related neurodegeneration. We further expect that WM concentrations will be lower in subjects with abnormal CSF values since amyloid and tau pathologies have shown pernicious effects on WM integrity from early AD stages (Hertze et al., 2013; Gold et al., 2014; Dean et al., 2017). Additionally, we have applied a graph theoretical approach to compare topological organization of cortical thickness networks between subjects with and without abnormal CSF levels. Our prediction is that $A\beta_{1-42}^{+}$ and p-tau^{+} individuals will present more segregated cortical networks, this effect being more evident in those regions where the Aβ load and neurodegeneration occur earlier in

AD (i.e., parietal and temporal lobes, respectively). Evidence suggests that the loss of integration in structural cortical networks appears late in AD (He et al., 2008; Romero-Garcia et al., 2016; see Tijms et al., 2016 for opposite results). Therefore, we expect that CN elderly subjects with abnormal CSF levels will show more segregated GM cortical networks while maintaining unaltered their integration capability.

2. Materials and Methods

2.1. Subjects

The study sample consisted of 57 CN elderly volunteers recruited at the Hospital Santa Creu i Sant Pau (Barcelona, Spain) and the University Hospital Marqués de Valdecilla (Santander, Spain), as part of a cross-sectional multicenter study called "SIGNAL project" (https://www.signalstudy.es/en/). Participants underwent neurological and neuropsychological evaluation (i.e., Mini Mental State Examination, Boston Naming Test, Clock Test, CERAD Word List, Rey-Osterrieth Complex Figure Test, and the Visual Object and Space Perception Battery). All of them showed normal cognitive performance relative to appropriate reference values for age and education (see Table 1), global CDR score of 0 (no dementia), as well as normal independent function. Subjects gave their informed consent prior to their inclusion in the study, which was approved by the local ethics committee at each center. Participants were grouped into controls (N=20) if they revealed normal CSF $A\beta_{1\text{-}42}$ ($\geq$ 550 pg/mL) and p-tau (< 61 pg/mL) levels, $A\beta_{1\text{-}42}{}^{+}$ (N=19) if they showed abnormal $A\beta_{1\text{-}42}$ (< 550 pg/mL) and normal p-tau levels, and p-tau^{+} (N=18) if they presented abnormal p-tau ($\geq$ 61 pg/mL) and normal $A\beta_{1\text{-}42}$ levels.

2.2. CSF measures

CSF was obtained through lumbar puncture and collected following international consensus recommendations (Alcolea et al., 2015). Briefly, CSF was collected in the morning between 09:00 and 12:00 hours in polypropylene tubes and immediately centrifuged for 10 min (1900-2000g). The first 1-2 cc were discarded to avoid hematic contamination. CSF samples were aliquoted (0.5 mL) into polypropylene tubes and frozen at -80°C. All CSF samples were shipped in dry ice to the Hospital Santa Creu i Sant Pau, where they were analyzed. Commercially available enzyme-linked immunosorbent assay (ELISA) kits were used to determine levels of $A\beta_{1\text{-}42}$ (Innotest β-amyloid$_{1–42}$; Fujirebio Europe) and p-tau (Innotest Phospho-Tau$_{181P}$; Fujirebio Europe), following the manufacturer's recommendations.

2.3. MRI acquisition

Participants were scanned in two different centers (Hospital Santa Creu i Sant Pau and University Hospital Marqués de Valdecilla) using the same protocol and identical MRI scanners (Philips Achieva 3T, 8-channel head coil). High-resolution structural scans were obtained with a T1-weighted magnetization-prepared rapid gradient echo sequence (1 mm^3 voxel size, no gap between slices, repetition time = 8.2 ms, echo-time = 3.8 ms, flip angle = 8º, matrix size = 240 x 234). Neuroimaging analyses were performed in the Laboratory of Functional Neuroscience at the Pablo de Olavide University (Seville, Spain).

2.4. Cortical thickness estimation

Cortical thickness was estimated using surface-based methods with analysis tools implemented in Freesurfer v5.3 (http://surfer.nmr.mgh.harvard.edu/), which have previously been validated against histological data (Rosas et al., 2002) and manual

segmentation (Kuperberg et al., 2003; Salat et al., 2004). The Freesurfer analysis pipeline involves intensity normalization, registration to Talairach space, skull stripping, WM segmentation, tesselation of the WM boundary, and automatic correction of topological defects (Fischl and Dale, 2000). Pial/WM boundaries were manually corrected on a slice-by-slice basis in each participant to increase the reliability of cortical thickness measurements. Special attention was paid to cortical regions at the border with the CSF to avoid partial volume effects. Cortical thickness maps were smoothed using non-linear spherical wavelet-based de-noising schemes, which have proved to enhance specificity and sensitivity at detecting local and global changes in cortical thickness (Bernal-Rusiel et al., 2008).

2.5. GM and WM volume estimation

The volume of cortical GM and cerebral WM was separately assessed using the voxel-based morphometry (VBM) approach integrated in SPM12 (Wellcome Trust Center for Neuroimaging; www.fil.ion.ucl.ac.uk/spm). Briefly, T1-weighted brain images were manually reoriented to the anterior commissure and further segmented into different compartments using the unified segmentation approach implemented in SPM12. Next, the diffeomorphic anatomical registration through an exponentiated lie algebra (DARTEL) algorithm was applied to segmented brain images to obtain an enhanced inter-subject registration with improved realignment of smaller inner structures (Ashburner, 2007). GM and WM maps were spatially normalized into the Montreal Neurological Institute (MNI) brain space (voxel size = 1.5 mm^3), and smoothed with an isotropic Gaussian kernel of 12 mm full-width at half-maximum. Group differences in WM were located in specific WM tracts using the JHU white-matter tractography atlas (Hua et al., 2008).

2.6. Estimation of cortical thickness networks and topological properties

Many real complex systems exhibit small world properties characterized by a high density of local connections (i.e., network segregation) together with a scarce number of links between distant regions (i.e., network integration), leading to highly efficient networks with a relatively low wiring cost and optimal adaptability to a broad range of circumstances (Travers and Milgram, 1969). Topological properties of cortical thickness networks have provided novel insights into the organizational principles of the human neocortex (He et al., 2007; Bassett et al., 2008; Chen et al., 2008; Lv et al., 2010). Correlated changes in cortical thickness have been used to assess the total correlation strength at every point in the cortex, and to investigate spatial differences in cross-cortical correlations between groups of subjects (Lerch et al., 2006). It has been hypothesized that networks of cortical thickness covariance may arise from genetic influences on normal development and aging, mutual trophic reinforcement as well as experience-related plasticity (Evans, 2013).

The analysis pipeline used here to obtain topological properties of cortical thickness networks has been described in detail elsewhere (Romero-Garcia et al., 2012; 2014). Briefly, we have employed a cortical scheme comprising 599 regions (250 mm^2 each) that has shown a good trade-off between small-world attributes and the number of regions in cortical thickness networks (Romero-Garcia et al., 2012). Next, partial correlations of interregional cortical thickness, adjusted by age, were used to build the thickness-based cortical network. Covariance patterns of cortical thickness were modelled through weighted graphs to encode the strength of connections between cortical regions. Correlations exceeding the statistical threshold (corrected p-value<0.05) were considered as significant connections in the cortical thickness network obtained for each group (i.e., controls, $A\beta_{1\text{-}42}^{+}$ and p-tau^{+}).

In the present study, the *weighted clustering coefficient* of the cortical thickness network (C_p) was computed as the likelihood whether the neighboring nodes are connected with each other (Onnela et al., 2005):

$$C_p = \frac{1}{N} \sum_{j,k \in G} \frac{\left(w_{ij} w_{jk} w_{ik}\right)^{1/3}}{\left(k_i \left(k_i - 1\right)/2\right)}$$

where N is the number of regions, w_{ij} is the weight connection between region i and j, and k_i is the degree of node i.

The *weighted path length* was defined as the average minimum travel distance that links any two nodes of the network, considered as the inverse of the weights of the connections (Newman, 2003):

$$L_p = \frac{1}{\frac{1}{N(N-1)} \sum_{i,j}^{N} \left(\frac{1}{L_{ij}}\right)}$$

where L_{ij} is the inverse of the edge weight ($L_{ij} = 1/w_{ij}$).

To determine lobe connectivity, we computed the *inward/outward lobe connectivity strength* (S_l) in each cortical lobe separately (i.e., frontal, central, parietal, temporal, occipital, and cingulate cortex) (Romero-Garcia et al., 2016):

$$S_l = \frac{1}{2} \sum_{ij} w_{ij}$$

where S_l is the sum of weights of the lobe (l) separated into four categories: (*i*) S_l^{in} reveals connections between regions that belongs to l, (*ii*) S_l^{intraH} shows connections from l to nodes out of l with the endpoint in the same hemisphere, (*iii*) S_l^{interH} refers to connections from l that cross to the opposite hemisphere, and (*iv*) $S_l^{in/out} = S_l^{in}/(S_l^{intraH} + S_l^{interH})$ shows the preference of l for inward connectivity opposed to connections that leave l.

A more detailed explanation of the above-mentioned network metrics is found elsewhere (Rubinov and Sporns, 2010). Network metrics may be influenced by characteristics of the network structure, such as the number of nodes and the amount of weights within the graph, making group comparisons problematic. To counteract these effects, 100 random networks with similar properties to the real network were built permuting all the network weights in each group (Maslov and Sneppen, 2002). This process preserves the nodes and the sum of weights but not the degree distribution. Finally, each metric was normalized by dividing the real value by the average across the 100 randomly rewired networks.

2.7. Statistical analysis

Statistical analyses were performed with SPSS v22 (SPSS Inc. Chicago, IL). We first assessed the normality assumption of all variables with the Shapiro-Wilk test. Demographic, cognitive and CSF data were normally distributed, allowing us to use parametric statistical tests with these variables. Group differences in demographic characteristics and cognitive performance were assessed with unpaired t-tests, with the exception of gender and ApoE ε4 distribution that was compared with the chi-square test.

Group differences in cortical thickness were assessed with an analysis of covariance (ANCOVA) performed in each hemisphere, with group as the main factor and age as nuisance. **The ApoE ε4 was not included as nuisance because its contribution was not significant.** Results were corrected for multiple comparisons using a previously validated hierarchical statistical model (Bernal-Rusiel et al., 2010). This procedure first controls the family wise error (FWE) rate at the level of clusters ($p<0.05$) by applying random field theory over smoothed statistical maps; and next controls the false

discovery rate (FDR) at the level of vertex ($p<0.05$) over unsmoothed statistical maps limited to significant clusters. The interaction between $A\beta_{1\text{-}42}^{+}$ and p-tau^{+} could not be tested due to the small number of participants (N=5) who showed abnormal concentrations in the two CSF markers.

Voxel-wise group differences of cortical GM and cerebral WM were assessed using ANCOVAs with age as nuisance. Statistical maps were thresholded at $p<0.05$ at the cluster level using the FWE rate.

As the distribution of the different network metrics is unknown, nonparametric permutation tests were used to assess group differences for each normalized metric derived from cortical thickness networks. Briefly, for each pair of groups (controls *versus* $A\beta_{1\text{-}42}^{+}$, controls *versus* p-tau^{+}, $A\beta_{1\text{-}42}^{+}$ *versus* p-tau^{+}), each subject was randomly reallocated to one of the two groups. Based on the randomly resampled subjects, network metrics were calculated using the same procedure as with the original data. Differences between metrics across permutations (N=10,000) were computed to build a reference distribution, and the 95th percentile value of this distribution was taken as the statistical threshold to retain or reject the null hypothesis of no group differences for each metric. In the particular case of the lobe connectivity metric, the inward/outward lobe connection strength was computed in different lobes for the left and right hemisphere separately. The multiple testing issue was counteracted employing a unique reference distribution collecting, for each permutation, the maximum square of metric differences. If the square of the original metric was higher than the 95th percentile of the maximum values of differences, it was considered statistically significant after controlling for the FWE rate (Maris, 2004).

3. Results

3.1. Demographic characteristics and cognitive functioning

Table 1 contains descriptive information of demographic, cognitive and CSF data in each group. All groups were comparable in sex distribution and education years, but p-tau$^+$ subjects were significantly older than controls (p=0.001). Scores derived from the neuropsychological evaluation did not differ among groups. Ranges of CSF values for each group were as follows: controls ($A\beta_{1\text{-}42}$: 764-1063.5 pg/mL; p-tau: 30-45 pg/mL), $A\beta_{1\text{-}42}^+$ ($A\beta_{1\text{-}42}$: 322-533.5 pg/mL; p-tau: 18-55.5 pg/mL), and p-tau$^+$ (p-tau: 61.5-132.5 pg/mL; $A\beta_{1\text{-}42}$: 583.5-1055.5 pg/mL).

3.2. Effects of abnormal CSF biomarkers on cortical thickness

Table 2 and Figure 1 show significant group differences in surface-based cortical thickness measures. Relative to controls, $A\beta_{1\text{-}42}^+$ individuals exhibited thickening of left middle temporal regions ($p=10^{-4}$), while p-tau$^+$ subjects showed cortical thinning in medial orbitofrontal regions ($p=10^{-4}$) as well as in the left superior parietal lobe ($p=10^{-5}$) and right precuneus ($p=10^{-3}$).

3.3. Effects of abnormal CSF biomarkers on GM and WM volume

No group differences were found in cortical GM volume. Table 3 and Figure 2 show significant group differences in voxel-based measurements of WM volume. Compared with controls, $A\beta_{1\text{-}42}^+$ subjects showed lower WM volume in the left parahippocampal cingulum that extended to forceps major ($p=10^{-4}$) and right subgenual cingulum (p=0.004). The loss of WM integrity was also evident in p-tau$^+$ subjects in the parahipocampal cingulum ($p=10^{-5}$) and uncinate fasciculus of the left hemisphere that further extended to regions of the inferior longitudinal fasciculus (p=0.003).

3.4. Effects of abnormal CSF biomarkers on the topology of cortical thickness networks

Figure 3 displays group differences in the topological organization of cortical thickness networks. Table 4 depicts group differences in inward/outward connectivity strength for each cortical lobe. Both $A\beta_{1\text{-}42}^{+}$ and p-tau^{+} individuals exhibited cortical thickness networks significantly more segregated than controls as revealed by the C_p metric (p=0.0004 and p=0.0001, respectively). Lobular isolation reflected in the *inward/outward* connectivity metric was higher in $A\beta_{1\text{-}42}^{+}$ subjects than in controls (p=0.01), likely due to the significant segregation of the left cingulate cortex (p=0.03) and the right temporal lobe (p=0.04). The lack of significant differences for the L_p metric indicated that abnormal levels of CSF biomarkers did not influence integration of cortical thickness networks in CN elderly subjects.

4. Discussion

The present study investigated whether abnormal CSF concentrations of $A\beta_{1\text{-}42}$ or p-tau in CN elderly are associated with structural changes in different brain compartments (cortical thickness and WM volume) and/or with variations in the topological organization of cortical thickness networks. Results revealed that the pattern of cortical thickness is biomarker specific. In particular, we found that cortical thickness was increased in $A\beta_{1\text{-}42}^{+}$ subjects in middle temporal regions but decreased in p-tau^{+} individuals in fronto-parietal regions. Abnormal CSF values of the two biomarkers appeared associated with WM atrophy in antero-posterior regions of the cingulum bundle and with more segregated cortical networks. In the particular case of $A\beta_{1\text{-}42}^{+}$ individuals, network segregation was further accompanied by increased isolation of temporal and cingulate regions. Collectively, these results highlight the relevance of

combining CSF measures with structural neuroimaging and connectomics to better define the landscape of brain changes in CN elderly subjects at risk for AD.

4.1. Abnormal CSF measures and cortical thickness in CN elderly

Here, we have shown that $A\beta_{1-42}^{+}$ subjects exhibited cortical thickening of middle temporal regions, supporting the hypothesis that cerebral amyloidosis without evidence of neurodegeneration is associated with pathological increases of cortical thickness in CN older adults (Fortea et al., 2014). Previous studies have linked abnormal CSF biomarkers to variations in cortical thickness in CN elderly subjects with contradictory results, likely due to differences in the criteria for establishing preclinical AD. In one of these studies, $A\beta_{1-42}^{+}$ individuals evidenced thickening of middle temporal and inferior parietal regions, whereas the interaction between $A\beta_{1-42}^{+}$ and p-tau^{+} led to regional patterns of cortical thinning (Fortea et al., 2014). Evidence suggests that pathological cortical thickening occurs long before the onset of clinical AD symptoms (Chetelat et al., 2010; Fortea et al., 2010; 2011; 2014 Johnson et al., 2014), which has been interpreted as brain reserve or other compensatory processes in response to toxic effects of Aβ oligomers or diffuse plaques (Chetelat et al., 2010). Furthermore, asymptomatic presenilin-1 (PSEN1) mutation carriers showed increased thickness in the precuneus and parietotemporal cortices (Fortea et al., 2010) and accelerated rates of cortical thinning in fronto-parieto-temporal regions (Sala-Llonch et al., 2015). Although the neurobiological substrate of cortical thickening in CN $A\beta_{1-42}^{+}$ elderly subjects is far from being understood, *post mortem* brain studies have found that asymptomatic subjects with amyloid plaques had hypertrophy of neuronal cell bodies, nuclei, and nucleoli (Iacono et al., 2008). These cellular changes have also been observed in transgenic AD mouse models, indicating that overexpression of amyloid precursor protein is necessary and sufficient for hypertrophy of cortical neurons (Oh et al., 2009),

and may indeed represent a very early reaction to cerebral amyloidosis or result from the activation of cellular processes in an attempt to prevent the natural progression of AD (Iacono et al., 2008). Therefore, converging lines of evidence suggest that cortical hypertrophy is potentially feasible at least during initial amyloidosis in asymptomatic elderly subjects.

Tau proteins are abundant in the cerebral cortex, appearing in regions that accumulate NFT as well as in other regions where NFT are not present (Trojanowski et al., 1989). High concentrations of CSF p-tau have been associated with cognitive decline in MCI (Buerger et al., 2002) and with neocortical NFT-pathology in AD patients (Buerger et al., 2006). Other studies have further shown that abnormal CSF tau biomarkers in CN elderly subjects are associated with hypometabolism in parietal regions (Petrie et al., 2009) and reduced cerebral blood flow in parietal, temporal, and frontal lobes (Stomrud et al., 2012), likely boosting synaptic dysfunctions and disconnection of cortical hubs caused by Aβ depositions (Drzezga et al., 2011).

It has been proposed that individuals with evidence of neurodegeneration but normal levels of $A\beta_{1\text{-}42}$ might be classified as having suspected non-Alzheimer pathology (SNAP), this condition occurring in 23% of CN individuals older than 65 years (Jack et al., 2012). There is currently intense debate about whether SNAP is a primary age-associated tauopathy (Crary et al., 2014) or represents an invariant feature of AD (Duyckaerts et al., 2015). Prospective studies have shown that 42% of the $A\beta_{1\text{-}42}^{+}$ subjects had SNAP at baseline and later transitioned to MCI/AD (Jack et al., 2013). Our results revealed that p-tau^{+} individuals exhibited cortical thinning in superior parietal regions bilaterally and in medial aspects of the left orbitofrontal cortex. Whether these p-tau^{+}-related patterns of cortical thinning are part of normal aging processes, other non-AD neurodegenerative disorders or represent part of the AD spectrum remains to

be determined in longitudinal studies with SNAP individuals using tau PET imaging combined with changes in cortical thickness. Beyond this question, and given that SNAP is relatively prevalent in the normal population (Jack et al., 2012), our cortical thickness results may have implications for the follow-up of SNAP in clinical settings and/or serve as surrogate of the evolution CN subjects with positive markers of neurodegeneration.

Most of our cortical thickness findings were circumscribed to the left hemisphere, replicating previous observations in MCI and AD patients using either VBM (Chetelat et al., 2002; Thompson et al., 2003; Karas et al., 2004) or surface-based cortical thickness analysis (e.g., Lerch et al., 2005; Singh et al., 2006). Longitudinal studies showed that left GM loss of medial temporo-parietal regions was strongly correlated with worse cognitive performance and faster leftward reduction of GM loss rates in AD patients, supporting a left lateralized acceleration of GM degeneration with advancing AD (Thompson et al., 2003). Clinico-pathological studies have also revealed a marked left predominance for vascular lesions not only in demented but also in CDR 0 cases, suggesting that vascular burden in the left hemisphere may remain cognitively silent while the right hemisphere is not invaded by AD lesions (Giannakopoulos et al., 2009).

Changes in surface-based cortical thickness observed in CN subjects with abnormal CSF levels of $A\beta_{1-42}$ and p-tau could not be replicated using volume-based analysis of GM density. Several reasons may account for this disparity of results. First, estimation of cortical thickness has demonstrated to provide a more sensitive measure of age-related decline in cortical GM compared with VBM techniques (Hutton et al., 2009). Second, VBM approaches seem to be less accurate than surface-based cortical thickness analysis, likely due to the limited resolution of the voxel grid. Furthermore, they are less robust to noise, and are significantly affected by partial volume effects at the boundaries

of convoluted structures such as deep sulci (Acosta et al., 2009). Finally, VBM analysis is sensitive to T1 signal variations, likely due to bias correction, an issue that does not occur with surface-based cortical thickness estimation methods (Chung et al., 2017).

4.2. Abnormal CSF measures and WM volume in CN elderly

Evidence of selective WM shrinkage in nondemented patients with histopathological lesions of AD was provided nearly three decades ago, suggesting that WM degeneration is likely due to cytoskeletal abnormalities associated with axonal degeneration (de la Monte, 1989). To date only a few studies have assessed WM alterations in CN elderly subjects with positive AD CSF biomarkers, and all of them were focused on changes in the WM microstructure using diffusion tensor imaging (Gold et al., 2014; Melah et al., 2016; Hoy et al., 2017). Some of these studies showed a widespread pattern of affected regions including frontal, parietal, and especially temporal WM (Gold et al., 2014; Hoy et al., 2017), whereas others reported focal patterns of WM damage in AD-related regions (Melah et al., 2016).

To our knowledge, results of the present study constitute the first *in vivo* evidence of morphometric WM atrophy in CN older adults with abnormal AD CSF measures. We found that p-tau^{+} subjects showed reduced concentrations of WM in the left uncinate fasciculus. The fiber bundles of the uncinate fasciculus originate in the WM of the temporal lobe, course around the middle cerebral artery, enter the extreme and external capsules, and continue into the orbitofrontal cortex (Kier et al., 2004). Interestingly, p-tau^{+} individuals further showed thinning of the left orbitofrontal cortex in our study, suggesting potential disruption in connectivity between frontal and inferior temporal cortex, which in turn has been postulated as a possible cause of memory impairment (Gaffan et al., 2002). Moreover, the uncinate fasciculus has a ventral part that connects

the orbitofrontal cortex with the hippocampus (Schneider et al., 1965), region that presents more accumulation of synaptic p-tau levels as compared to $A\beta_{1-42}$ (Fein et al., 2008).

The cingulum bundle forms a WM tract integrated by subgenual, retrosplenial, and parahippocampal subdivisions, each of these regions with different WM microstructure (Mufson and Pandya, 1984) that impact differently on the capacity of the WM to transmit electrical impulses (Beaulieu, 2002). Growing evidence suggests that the cingulum becomes especially vulnerable in different AD stages, affecting both posterior (Zhang et al., 2007; Chua et al., 2009; Delano-Wood et al., 2012) and anterior subdivisions (Rosenberg et al., 2013). In the present study, $A\beta_{1-42}^{+}$ and p-tau^{+} subjects exhibited lower WM volume in caudal parts of the cingulum, termed the "parahippocampal" portion because the large majority of fibers project to the medial temporal lobe (Jones et al., 2013), structure that has shown a rapid rate of atrophy in patients with histopathologically-confirmed AD (de Leon et al., 1993; Jobst et al., 1994).

Analysis further revealed reduced WM concentrations in the anterior part (subgenual) of the cingulum in $A\beta_{1-42}^{+}$ individuals as compared with controls. The subgenual cingulum projects the insula and amygdala (Klingler and Gloor, 1960), and receives cholinergic efferents from the diagonal band and medial septum (Selden et al., 1998). All these regions have shown to be considerably affected in MCI patients (Cantero et al., 2017), suggesting that the integrity loss of the subgenual cingulum may precede damage of their innervated GM regions. Moreover, previous studies have shown that greater amyloid load in anterior cingulate regions is associated with lower immediate recall in CN elderly subjects (Rosenberg et al., 2013), and those normal individuals with PET evidence of brain amyloid deposition have exhibited failures of functional connectivity

between the anterior cingulate and the hippocampus. Overall, our results support the potential involvement of the cingulum bundle in preclinical AD, and provide evidence of regional effects on this limbic structure due to cerebral amyloidosis or SNAP.

4.3. CSF measures and topological organization of cortical thickness networks in CN elderly

Topological properties of thickness-based cortical networks have provided evidence for disrupted structural networks in normal aging (Chen et al., 2011; Wu et al., 2012; Romero-Garcia et al., 2014) and different AD stages (He et al., 2008; Romero-Garcia et al., 2016). Our study extends this knowledge to CN elderly subjects with abnormal CSF measures of $A\beta_{1-42}$ and p-tau, revealing that intrinsic changes in the topology of morphometric cortical networks may be helpful in monitoring AD lesions in asymptomatic subjects. We found that individuals with abnormal CSF biomarkers of AD showed cortical thickness networks significantly more segregated (i.e., weakened interregional relationships in morphometric networks) without alterations in network integration. Previous studies have shown that disrupted integration in structural networks mainly occurs in clinical AD stages characterized by impaired cognition (He et al., 2008; Romero-Garcia et al., 2016), indicating that higher clustering combined with longer path lengths in MCI/AD reflect reduced network efficiency likely due to synaptic dysfunctions and neuronal loss observed in prodromal and clinical AD stages. This does not mean, however, that both isolation and loss of integration occur simultaneously. Very likely, increasing segregation progressively leads to integration disruption and subsequent cognitive impairment. In line with this hypothesis, our asymptomatic elderly subjects with cerebral amyloidosis or incipient neurodegeneration showed lobular segregation and preserved network integration.

We further showed that pathological levels of CSF $A\beta_{1-42}$ specifically contributed to the isolation of the temporal and cingulate cortices. Both regions suffer a progressive reduction in cortical acetylcholinesterase-rich fibers from normal aging to AD (Geula and Mesulam, 1989), being targets for the widest range of AD lesions (Brun and Englund, 1981), and showing connectivity failures (Sorg et al., 2007; Stam et al., 2007) and decreased topological centrality in AD patients (He et al., 2008). Furthermore, temporal and cingulate structures are canonical components of the default mode network (Buckner et al., 2008), which has shown to be affected in CN elderly subjects with positive AD markers (Sheline et al., 2010; Lim et al., 2014; Oh et al., 2014). Overall, these results suggest that global effects of incipient AD lesions may also be disclosed considering the neocortex as a complex network and studying its topological features at different organization levels.

5. Conclusions

Asymptomatic older adults presenting abnormal CSF concentrations of either $A\beta_{1-42}$ or p-tau showed similar loss of WM integrity, augmented isolation of cortical regions and no changes in network integration, the latter likely accounts for the lack of cognitive impairment. Abnormal levels of each CSF biomarker were associated with specific patterns of cortical thickness, which is coherent with the idea that different mechanisms underlie amyloidosis and neurodegeneration in asymptomatic older adults at risk for AD. Future longitudinal studies should determine whether this combination of markers is able to detect potential candidates for intervention with disease-modifying therapies aimed at slowing or halting the progression of AD.

Acknowledgments

This work was supported by research grants from the Spanish Ministry of Economy and Competitiveness (SAF2011-25463 to J.L.C., PSI2014-55747-R to M.A.), the Carlos III Institute of Health, Spain (PI11/02425 and PI14/01126 to J.F.; PI11/3035 and PI14/1561 to A.L.; PI08/0139, PI12/02288 and PI16/01652 to P.S.J.), jointly funded by Fondo Europeo de Desarrollo Regional (FEDER), Unión Europea, "Una manera de hacer Europa", the Joint Programming in Neurodegenerative Disease Research (DEMTEST to P.S.J.), "Marató TV3" (project 20141210 to J.F. and 20142610 to A.L.), the Regional Ministry of Innovation, Science and Enterprise, Junta de Andalucia (P12-CTS-2327 to J.C.L.), and the CIBERNED program (Signal project).

Figure legends

Figure 1. Changes in cortical thickness in CN elderly subjects with abnormal CSF levels of $A\beta_{1-42}$ or p-tau. A. Significant patterns of cortical changes were represented on inflated cortical surfaces. Color bars represent corrected p-values ($p<0.05$) using a hierarchical approach based on sequential statistical thresholding (Bernal-Rusiel et al., 2010). B. Significant patterns of cortical thickness changes are also displayed on flattened cortical surfaces. Squares with colored borders limit the location of significant regional changes. C. The surface of the square was zoomed on flattened cortical maps displaying cytoarchitectonic delimitation of affected regions. *Abbreviations for the left middle temporal cortex (squares with yellow borders)*: TA – primary auditory cortex; TAr – rostral auditory cortex; TG – temporopolar area; TAp – polysensory cortex; TE – temporal area; TEd – temporal dorsal area; iTC – inferior temporal cortex; FG – fusiform gyrus; PG – angular gyrus (McDonald et al., 2000; Ding et al., 2009). *Abbreviations for the left medial orbitofrontal cortex (square with blue border)*: B11 – medial portion of ventral frontal lobe; cg – cingulate gyrus; Fp2 – medial frontopolar area 2; fms – frontomarginal sulcus; SFG – superior frontal gyrus; (Bludau et al., 2014). *Abbreviations for the left superior parietal cortex and right precuneus (square with blue and green border, respectively)*: CiS – cingulate sulcus; CPD – cingulate postdorsal; CPV – cingulate postventral; PrC – precuneus; SuPS – subparietal sulcus; CS – central sulcus; POS – parieto-occipital sulcus; PCL – posterior paracentral lobule (Scheperjans et al., 2008); hOc4lp – posterior occipital, area 4; hOc4d – dorsal occipital, area 4 (Malikovic et al., 2016).

Figure 2. Patterns of WM atrophy in CN elderly subjects with abnormal CSF levels of $A\beta_{1-42}$ or p-tau. A. $A\beta_{1-42}^{+}$ subjects showed lower concentration of WM volume in the

left cingulum parahippocampal and right subgenual cingulum. B. p-tau^{+} subjects exhibited lower concentration of WM volume in the left cingulum parahippocampal and left uncinate fasciculus. Location of affected WM regions were obtained with the JHU white-matter tractography atlas (Hua et al., 2008).

Figure 3. Disrupted cortical thickness networks in CN elderly subjects with abnormal CSF levels of $A\beta_{1\text{-}42}$ or p-tau. A. Group differences in network segregation in the whole-cortex (left panel) and at lobular (right panel) level. B. Network segregation in those cortical lobes where group differences reached statistical significance. The right panel displays the cortical lobe affected after statistical comparisons (see left panel). $^{**}p_{corrected}<0.005$; $^{*}p_{corrected}<0.01$

References

Acosta, O., Bourgeat, P., Zuluaga, M.A., Fripp, J., Salvado, O., Ourselin, S.; Alzheimer's Disease Neuroimaging Initiative, 2009. Automated voxel-based 3D cortical thickness measurement in a combined Lagrangian-Eulerian PDE approach using partial volume maps. Med Image Anal. 13, 730-743.

Alcolea, D., Martínez-Lage, P., Sánchez-Juan, P., Olazarán, J., Antúnez, C., Izagirre, A., Ecay-Torres, M., Estanga, A., Clerigué, M., Guisasola, M.C., Sánchez Ruiz, D., Marín Muñoz, J., Calero, M., Blesa, R., Clarimón, J., Carmona-Iragui, M., Morenas-Rodríguez, E., Rodríguez-Rodríguez, E., Vázquez Higuera, J.L., Fortea, J., Lleó, A., 2015. Amyloid precursor protein metabolism and inflammation markers in preclinical Alzheimer disease. Neurology 85, 626-633.

Arenaza-Urquijo, E.M., Molinuevo, J.L., Sala-Llonch, R., Solé-Padullés, C., Balasa, M., Bosch, B., Olives, J., Antonell, A., Lladó, A., Sánchez-Valle, R., Rami, L., Bartrés-Faz, D., 2013. Cognitive reserve proxies relate to gray matter loss in cognitively healthy elderly with abnormal cerebrospinal fluid amyloid-β levels. J Alzheimers Dis. 35, 715-726.

Ashburner, J., 2007. A fast diffeomorphic image registration algorithm. Neuroimage 38, 95-113.

Bassett, D.S., Bullmore, E., Verchinski, B.A., Mattay, V.S., Weinberger, D.R., Meyer-Lindenberg, A., 2008. Hierarchical organization of human cortical networks in health and schizophrenia. J Neurosci. 28, 9239-9248.

Bateman, R.J., Xiong, C., Benzinger, T.L., Fagan, A.M., Goate, A., Fox, N.C., Marcus, D.S., Cairns, N.J., Xie, X., Blazey, T.M., Holtzman, D.M., Santacruz, A., Buckles, V.,

Oliver, A., Moulder, K., Aisen, P.S., Ghetti, B., Klunk, W.E., McDade, E., Martins, R.N., Masters, C.L., Mayeux, R., Ringman, J.M., Rossor, M.N., Schofield, P.R., Sperling, R.A., Salloway, S., Morris, J.C.; Dominantly Inherited Alzheimer Network, 2012. Clinical and biomarker changes in dominantly inherited Alzheimer's disease. N Engl J Med. 367, 795-804.

Beaulieu, C., 2002. The basis of anisotropic water diffusion in the nervous system - a technical review. NMR Biomed. 15, 435-455.

Becker, J.A., Hedden, T., Carmasin, J., Maye, J., Rentz, D.M., Putcha, D., Fischl, B., Greve, D.N., Marshall, G.A., Salloway, S., Marks, D., Buckner, R.L., Sperling, R.A., Johnson, K.A., 2011. Amyloid-β associated cortical thinning in clinically normal elderly. Ann Neurol. 69, 1032-1042.

Bernal-Rusiel, J.L., Atienza, M., Cantero, J.L., 2008. Detection of focal changes in human cortical thickness: spherical wavelets versus Gaussian smoothing. Neuroimage 41, 1278-1292.

Bernal-Rusiel, J.L., Atienza, M., Cantero, J.L., 2010. Determining the optimal level of smoothing in cortical thickness analysis: a hierarchical approach based on sequential statistical thresholding. Neuroimage 52, 158-171.

Blennow, K., Hampel, H., 2003. CSF markers for incipient Alzheimer's disease. Lancet Neurol. 2, 605-613.

Bludau, S., Eickhoff, S.B., Mohlberg, H., Caspers, S., Laird, A.R., Fox, P.T., Schleicher, A., Zilles, K., Amunts, K., 2014. Cytoarchitecture, probability maps and functions of the human frontal pole. Neuroimage 93 Pt 2, 260-275.

Bobinski, M., de Leon, M.J., Wegiel, J., Desanti, S., Convit, A., Saint Louis, L.A., Rusinek, H., Wisniewski, H.M., 2000. The histological validation of post mortem magnetic resonance imaging-determined hippocampal volume in Alzheimer's disease. Neuroscience 95, 721-725.

Brun, A., Englund, E., 1981. Regional pattern of degeneration in Alzheimer's disease: neuronal loss and histopathological grading. Histopathology 5, 549-564.

Buckner, R.L., Andrews-Hanna, J.R., Schacter, D.L., 2008. The brain's default network: anatomy, function, and relevance to disease. Ann N Y Acad Sci. 1124, 1-38.

Buerger, K., Teipel, S.J., Zinkowski, R., Blennow, K., Arai, H., Engel, R., Hofmann-Kiefer, K., McCulloch, C., Ptok, U., Heun, R., Andreasen, N., DeBernardis, J., Kerkman, D., Moeller, H., Davies, P., Hampel, H., 2002. CSF tau protein phosphorylated at threonine 231 correlates with cognitive decline in MCI subjects. Neurology 59, 627-629.

Buerger, K., Ewers, M., Pirttilä, T., Zinkowski, R., Alafuzoff, I., Teipel, S.J., DeBernardis, J., Kerkman, D., McCulloch, C., Soininen, H., Hampel, H., 2006. CSF phosphorylated tau protein correlates with neocortical neurofibrillary pathology in Alzheimer's disease. Brain 129, 3035-3041.

Cantero, J.L, Zaborszky, L., Atienza, M., 2017. Volume loss of the nucleus basalis of Meynert is associated with atrophy of innervated regions in mild cognitive impairment. Cereb Cortex 27, 3881-3889.

Chen, Z.J., He, Y., Rosa-Neto, P., Germann, J., Evans, A.C., 2008. Revealing modular architecture of human brain structural networks by using cortical thickness from MRI. Cereb Cortex 18, 2374-2381.

Chen, Z.J., He, Y., Rosa-Neto, P., Gong, G., Evans, A.C., 2011. Age-related alterations in the modular organization of structural cortical network by using cortical thickness from MRI. Neuroimage 56, 235-245.

Chetelat, G., Desgranges, B., De La Sayette, V., Viader, F., Eustache, F., Baron, J.C., 2002. Mapping gray matter loss with voxel-based morphometry in mild cognitive impairment. Neuroreport 13, 1939-1943.

Chetelat, G., Villemagne, V.L., Pike, K.E., Baron, J.C., Bourgeat, P., Jones, G., Faux, N.G., Ellis, K.A., Salvado, O., Szoeke, C., Martins, R.N., Ames, D., Masters, C.L., Rowe, C.C.; Australian Imaging Biomarkers and Lifestyle Study of Ageing (AIBL) Research Group., 2010. Larger temporal volume in elderly with high versus low beta-amyloid deposition. Brain 133, 3349-3358.

Chua, T.C., Wen, W., Chen, X., Kochan, N., Slavin, M.J., Trollor, J.N., Brodaty, H., Sachdev, P.S., 2009. Diffusion tensor imaging of the posterior cingulate is a useful biomarker of mild cognitive impairment. Am J Geriatr Psychiatry 17, 602-613.

Chung, S., Wang, X., Lui, Y.W., 2017. Influence of T1-weighted signal intensity on FSL voxel-based morphometry and FreeSurfer cortical thickness. AJNR Am J Neuroradiol. 38, 726-728.

Crary, J.F., Trojanowski, J.Q., Schneider, J.A., Abisambra, J.F., Abner, E.L., Alafuzoff, I., Arnold, S.E., Attems, J., Beach, T.G., Bigio, E.H., Cairns, N.J., Dickson, D.W., Gearing, M., Grinberg, L.T., Hof, P.R., Hyman, B.T., Jellinger, K., Jicha, G.A., Kovacs, G.G., Knopman, D.S., Kofler, J., Kukull, W.A., Mackenzie, I.R., Masliah, E., McKee, A., Montine, T.J., Murray, M.E., Neltner, J.H., Santa-Maria, I., Seeley, W.W., Serrano-Pozo, A., Shelanski, M.L., Stein, T., Takao, M., Thal, D.R., Toledo, J.B., Troncoso,

J.C., Vonsattel, J.P., White, C.L., Wisniewski, T., Woltjer, R.L., Yamada, M., Nelson, P.T., 2014. Primary age-related tauopathy (PART): a common pathology associated with human aging. Acta Neuropathol. 128, 755-766.

Dean, D.C., Hurley, S.A., Kecskemeti, S.R., O'Grady, J.P., Canda, C., Davenport-Sis, N.J., Carlsson, C.M., Zetterberg, H., Blennow, K., Asthana, S., Sager, M.A., Johnson, S.C., Alexander, A.L., Bendlin, B.B., 2017. Association of amyloid pathology with myelin alteration in preclinical Alzheimer disease. JAMA Neurol. 74, 41-49.

De la Monte S.M., 2009. Quantitation of cerebral atrophy in preclinical and end-stage Alzheimer's disease. Ann Neurol. 25, 450-459.

Delano-Wood, L., Stricker, N.H., Sorg, S.F., Nation, D.A., Jak, A.J., Woods, S.P., Libon, D.J., Delis, D.C., Frank, L.R., Bondi, M.W., 2012. Posterior cingulum white matter disruption and its associations with verbal memory and stroke risk in mild cognitive impairment. J Alzheimers Dis. 29, 589-603.

de Leon, M.J., Golomb, J., Convit, A., DeSanti, S., McRae, T.D., George, A.E., 1993. Measurement of medial temporal lobe atrophy in diagnosis of Alzheimer's disease. Lancet 341, 125-126.

Ding, S.L., Van Hoesen, G.W., Cassell, M.D., Poremba, A., 2009. Parcellation of human termporal polar cortex: a combined analysis of multiple cytoarchitectonic, chemoarchitectonic, and phthological markers. J Comp Neurol. 514, 595-623.

Doherty, B.M., Schultz, S.A., Oh, J.M., Koscik, R.L., Dowling, N.M., Barnhart, T.E., Murali, D., Gallagher, C.L., Carlsson, C.M., Bendlin, B.B., LaRue, A., Hermann, B.P., Rowley, H.A., Asthana, S., Sager, M.A., Christian, B.T., Johnson, S.C., Okonkwo, O.C., 2015. Amyloid burden, cortical thickness, and cognitive

function in the Wisconsin Registry for Alzheimer's Prevention. Alzheimers Dement. 1, 160-169.

Drzezga, A., Becker, J.A., Van Dijk, K.R., Sreenivasan, A., Talukdar, T., Sullivan, C., Schultz, A.P., Sepulcre, J., Putcha, D., Greve, D., Johnson, K.A., Sperling, R.A., 2011. Neuronal dysfunction and disconnection of cortical hubs in non-demented subjects with elevated amyloid burden. Brain 134, 1635-1646.

Dugger, B.N., Hentz, J.G., Adler, C.H., Sabbagh, M.N., Shill, H.A., Jacobson, S., Caviness, J.N., Belden, C., Driver-Dunckley, E., Davis, K.J., Sue, L.I., Beach, T.G., 2014. Clinicopathological outcomes of prospectively followed normal elderly brain bank volunteers. J Neuropathol Exp Neurol. 73, 244-252.

Duyckaerts, C., Braak, H., Brion, J.P., Buée, L., Del Tredici, K., Goedert, M., Halliday, G., Neumann, M., Spillantini, M.G., Tolnay, M., Uchihara, T., 2015. PART is part of Alzheimer disease. Acta Neuropathol. 129, 749-756.

Evans, A.C., 2013. Networks of anatomical covariance. Neuroimage 80, 489-504.

Fagan, A.M., Roe, C.M., Xiong, C., Mintun, M.A., Morris, J.C., Holtzman, D.M., 2007. Cerebrospinal fluid tau/beta-amyloid42 ratio as a prediction of cognitive decline in nondemented older adults. Arch Neurol. 64, 343–349.

Fein, J.A., Sokolow, S., Miller, C.A., Vinters, H.V., Yang, F., Cole, G.M., Gylys, K.H., 2008. Co-localization of amyloid beta and tau pathology in Alzheimer's disease synaptosomes. Am J Pathol. 172, 1683-1692.

Fischl, B., Dale, A., 2000. Measuring the thickness of the human cerebral cortex from magnetic resonance images. Proc Natl Acad Sci USA 97, 11050-11055.

Fjell, A.M., Walhovd, K.B., Fennema-Notestine, C., McEvoy, L.K., Hagler, D.J., Holland, D., Blennow, K., Brewer, J.B., Dale, A.M.; Alzheimer's Disease Neuroimaging Initiative., 2010. Brain atrophy in healthy aging is related to CSF levels of Aβ1-42. Cereb Cortex 20, 2069-2079.

Fortea, J., Sala-Llonch, R., Bartrés-Faz, D., Bosch, B., Lladó, A., Bargalló, N., Molinuevo, J.L., Sánchez-Valle, R., 2010. Increased cortical thickness and caudate volume precede atrophy in PSEN1 mutation carriers. J Alzheimers Dis. 22, 909-922.

Fortea, J., Sala-Llonch, R., Bartrés-Faz, D., Lladó, A., Solé-Padullés, C., Bosch, B., Antonell, A., Olives, J., Sanchez-Valle, R., Molinuevo, J.L., Rami, L., 2011. Cognitively preserved subjects with transitional cerebrospinal fluid ß-amyloid 1-42 values have thicker cortex in Alzheimer's disease vulnerable areas. Biol Psychiatry 70, 183-190.

Fortea, J., Vilaplana, E., Alcolea, D., Carmona-Iragui, M., Sánchez-Saudinos, M.B., Sala, I., Antón-Aguirre, S., González, S., Medrano, S., Pegueroles, J., Morenas, E., Clarimón, J., Blesa, R., Lleó, A.; Alzheimer's Disease Neuroimaging Initiative., 2014. Cerebrospinal fluid β-amyloid and phospho-tau biomarker interactions affecting brain structure in preclinical Alzheimer disease. Ann Neurol. 76, 223-230.

Gaffan, D., Easton, A., Parker, A., 2002. Interaction of inferior temporal cortex with frontal cortex and basal forebrain: double dissociation in strategy implementation and associative learning. J Neurosci. 22, 7288-7296.

Geula, C., Mesulam, M.M., 1989. Cortical cholinergic fibers in aging and Alzheimer's disease: a morphometric study. Neuroscience 33, 469-481.

Giannakopoulos, P., Kövari, E., Herrmann, F.R., Hof, P.R., Bouras, C., 2009. Interhemispheric distribution of Alzheimer disease and vascular pathology in brain aging. Stroke 40, 983-986.

Gold, B.T., Zhu, Z., Brown, C.A., Andersen, A.H., LaDu, M.J., Tai, L., Jicha, G.A., Kryscio, R.J., Estus, S., Nelson, P.T., Scheff, S.W., Abner, E., Schmitt, F.A., Van Eldik, L.J., Smith, C.D., 2014. White matter integrity is associated with cerebrospinal fluid markers of Alzheimer's disease in normal adults. Neurobiol Aging 35, 2263-2271.

Gordon, B.A., Blazey, T., Su, Y., Fagan, A.M., Holtzman, D.M., Morris, J.C., Benzinger, T.L., 2016. Longitudinal β-amyloid deposition and hippocampal volume in preclinical Alzheimer disease and suspected non-Alzheimer disease pathophysiology. JAMA Neurol. 73, 1192-1200.

Hampel, H., Blennow, K., Shaw, L.M., Hoessler, Y.C., Zetterberg, H., Trojanowski, J.Q., 2010. Total and phosphorylated tau protein as biological markers of Alzheimer's disease. Exp Gerontol. 45, 30-40.

He, Y., Chen, Z.J., Evans, A.C., 2007. Small-world anatomical networks in the human brain revealed by cortical thickness from MRI. Cereb Cortex. 17, 2407-2419.

He, Y., Chen, Z., Evans, A., 2008. Structural insights into aberrant topological patterns of large-scale cortical networks in Alzheimer's disease. J Neurosci. 28, 4756-4766.

Hedden, T., Oh, H., Younger, A.P., Patel, T.A., 2013. Meta-analysis of amyloid-cognition relations in cognitively normal older adults. Neurology 80, 1341-1348.

Hertze, J., Palmqvist, S., Minthon, L., Hansson, O., 2013. Tau pathology and parietal white matter lesions have independent but synergistic effects on early development of Alzheimer's disease. Dement Geriatr Cogn Dis Extra. 3, 113-122.

Hoy, A.R., Ly, M., Carlsson, C.M., Okonkwo, O.C., Zetterberg, H., Blennow, K., Sager, M.A., Asthana, S., Johnson, S.C., Alexander, A.L., Bendlin, B.B., 2017. Microstructural white matter alterations in preclinical Alzheimer's disease detected using free water elimination diffusion tensor imaging. PLoS One 12(3):e0173982.

Hua, K., Zhang, J., Wakana, S., Jiang, H., Li, X., Reich, D.S., Calabresi, P.A., Pekar, J.J., van Zijl, P.C., Mori, S., 2008. Tract probability maps in stereotaxic spaces: analyses of white matter anatomy and tract-specific quantification. Neuroimage 39, 336-347.

Hutton, C., Draganski, B., Ashburner, J., Weiskopf, N., 2009. A comparison between voxel-based cortical thickness and voxel-based morphometry in normal aging. Neuroimage 48, 371-380.

Iacono, D., O'Brien, R., Resnick, S.M., Zonderman, A.B., Pletnikova, O., Rudow, G., An, Y., West, M.J., Crain, B., Troncoso, J.C., 2008. Neuronal hypertrophy in asymptomatic Alzheimer disease. J Neuropathol Exp Neurol. 67, 578-589.

Jack, C.R. Jr., Knopman, D.S., Weigand, S.D., Wiste, H.J., Vemuri, P., Lowe, V., Kantarci, K., Gunter, J.L., Senjem, M.L., Ivnik, R.J., Roberts, R.O., Rocca, W.A., Boeve, B.F., Petersen, R.C., 2012. An operational approach to National Institute on Aging-Alzheimer's Association criteria for preclinical Alzheimer disease. Ann Neurol. 71, 765-775.

Jack, C.R. Jr., Wiste, H.J., Weigand, S.D., Knopman, D.S., Lowe, V., Vemuri, P., Mielke, M.M., Jones, D.T., Senjem, M.L., Gunter, J.L., Gregg, B.E., Pankratz, V.S., Petersen, R.C., 2013. Amyloid-first and neurodegeneration-first profiles characterize incident amyloid PET positivity. Neurology 81, 1732-1740.

Jack, C.R. Jr., Wiste, H.J., Weigand, S.D., Rocca, W.A., Knopman, D.S., Mielke, M.M., Lowe, V.J., Senjem, M.L., Gunter, J.L., Preboske, G.M., Pankratz, V.S., Vemuri, P., Petersen, R.C., 2014. Age-specific population frequencies of cerebral β-amyloidosis and neurodegeneration among people with normal cognitive function aged 50-89 years: a cross-sectional study. Lancet Neurol. 13, 997-1005.

Jack, C.R. Jr., Bennett, D.A., Blennow, K., Carrillo, M.C., Feldman, H.H., Frisoni, G.B., Hampel, H., Jagust, W.J., Johnson, K.A., Knopman, D.S., Petersen, R.C., Scheltens, P., Sperling, R.A., Dubois, B., 2016. A/T/N: An unbiased descriptive classification scheme for Alzheimer disease biomarkers. Neurology 87, 539-547.

Jobst, K.A., Smith, A.D., Szatmari, M., Esiri, M.M., Jaskowski, A., Hindley, N., McDonald, B., Molyneux, A.J., 1994. Rapidly progressing atrophy of medial temporal lobe in Alzheimer's disease. Lancet 343, 829-830.

Johnson, S.C., Christian, B.T., Okonkwo, O.C., Oh, J.M., Harding, S., Xu, G., Hillmer, A.T., Wooten, D.W., Murali, D., Barnhart, T.E., Hall, L.T., Racine, A.M., Klunk, W.E., Mathis, C.A., Bendlin, B.B., Gallagher, C.L., Carlsson, C.M., Rowley, H.A., Hermann, B.P., Dowling, N.M., Asthana, S., Sager, M.A., 2014. Amyloid burden and neural function in people at risk for Alzheimer's Disease. Neurobiol Aging 35, 576-584.

Jones, D.K., Christiansen, K.F., Chapman, R.J., Aggleton, J.P., 2013. Distinct subdivisions of the cingulum bundle revealed by diffusion MRI fibre tracking: implications for neuropsychological investigations. Neuropsychologia 51, 67-78.

Karas, G.B., Burton, E.J., Rombouts, S.A., van Schijndel, R.A., O'Brien, J.T., Scheltens, Ph., McKeith, I.G., Williams, D., Ballard, C., Barkhof, F., 2003. A comprehensive study of gray matter loss in patients with Alzheimer's disease using optimized voxel-based morphometry. Neuroimage 18, 895-907.

Kier, E.L., Staib, L.H., Davis, L.M., Bronen, R.A., 2004. MR imaging of the temporal stem: anatomic dissection tractography of the uncinate fasciculus, inferior occipitofrontal fasciculus, and Meyer's loop of the optic radiation. AJNR Am J Neuroradiol. 25, 677-691.

Klingler, J., Gloor, P. The connections of the amygdala and of the anterior temporal cortex in the human brain. J Comp Neurol. 115, 333-369.

Knopman, D.S., Parisi, J.E., Salviati, A., Floriach-Robert, M., Boeve, B.F., Ivnik, R.J., Smith, G.E., Dickson, D.W., Johnson, K.A., Petersen, L.E., McDonald, W.C., Braak, H., Petersen, R.C., 2003. Neuropathology of cognitively normal elderly. J Neuropathol Exp Neurol. 62, 1087-1095.

Knopman, D.S., Jack, C.R. Jr., Wiste, H.J., Weigand, S.D., Vemuri, P., Lowe, V., Kantarci, K., Gunter, J.L., Senjem, M.L., Ivnik, R.J., Roberts, R.O., Boeve, B.F., Petersen, R.C., 2012. Short-term clinical outcomes for stages of NIA-AA preclinical Alzheimer disease. Neurology 78, 1576-1582.

Kuperberg, G.R., Broome, M.R., McGuire, P.K., David, A.S., Eddy, M., Ozawa, F., Goff, D., West, W.C., Williams, S.C., Van der Kouwe, A.J., Salat, D.H., Dale, A.M.,

Fischl, B., 2003. Regionally localized thinning of the cerebral cortex in schizophrenia. Arch Gen Psychiatry 60, 878-888.

Lerch, J.P., Pruessner, J.C., Zijdenbos, A., Hampel, H., Teipel, S.J., Evans, A.C., 2005. Focal decline of cortical thickness in Alzheimer's disease identified by computational neuroanatomy. Cereb Cortex 15, 995-1001.

Lerch, J.P., Worsley, K., Shaw, W.P., Greenstein, D.K., Lenroot, R.K., Giedd, J., Evans, A.C., 2006. Mapping anatomical correlations across cerebral cortex (MACACC) using cortical thickness from MRI. Neuroimage 31, 993-1003.

Lim, H.K., Nebes, R., Snitz, B., Cohen, A., Mathis, C., Price, J., Weissfeld, L., Klunk, W., Aizenstein, H.J., 2014. Regional amyloid burden and intrinsic connectivity networks in cognitively normal elderly subjects. Brain 137, 3327-3338.

Lv, B., Li, J., He, H., Li, M., Zhao, M., Ai, L., Yan, F., Xian, J., Wang, Z., 2010. Gender consistency and difference in healthy adults revealed by cortical thickness. Neuroimage 53, 373-382.

Malikovic, A., Amunts, K., Schleicher, A., Mohlberg, H., Kujovic, M., Palomero-Gallagher, N., Eickhoff, S.B., Zilles, K., 2016. Cytoarchitecture of the human lateral occipital cortex: mapping of two extrastriate areas hOc4la and hOc4lp. Brain Struct Funct. 221, 1877-1897.

Maris, E., 2004. Randomization tests for ERP topographies and whole spatiotemporal data matrices. Psychophysiology 41, 142-151.

Maslov, S., Sneppen, K., 2002. Specificity and stability in topology of protein networks, Science 296, 910-913.

Mattsson, N., Insel, P.S., Donohue, M., Jagust, W., Sperling, R., Aisen, P., Weiner, M.W.; Alzheimer's Disease Neuroimaging Initiative., 2015. Predicting reduction of cerebrospinal fluid β-amyloid 42 in cognitively healthy controls. JAMA Neurol. 72, 554-560.

McDonald, B., Highley, J.R., Walker, M.A., Herron, B.M., Cooper, S.J., Esiri, M.M., Crow, T.J., 2000. Anomalous asymmetry of fusiform and parahipocampal gyrus gray matter in schizophrenia: A postmortem study. Am J Psychiatry 157, 40-47.

Melah, K.E., Lu, S.Y., Hoscheidt, S.M., Alexander, A.L., Adluru, N., Destiche, D.J., Carlsson, C.M., Zetterberg, H., Blennow, K., Okonkwo, O.C., Gleason, C.E., Dowling, N.M., Bratzke, L.C., Rowley, H.A., Sager, M.A., Asthana, S., Johnson, S.C., Bendlin, B.B., 2016. Cerebrospinal fluid markers of Alzheimer's disease pathology and microglial activation are associated with altered white matter microstructure in asymptomatic adults at risk for Alzheimer's disease. J Alzheimers Dis. 50, 873-886.

Mufson, E.J., Pandya, D.N., 1984. Some observations on the course and composition of the cingulum bundle in the rhesus monkey. J Comp Neurol. 225, 31-43.

Newman, M.E.J., 2003. The structure and function of complex networks. SIAM Rev. 45, 167-168.

Onnela, J.P., Saramäki, J., Kertész, J., Kaski, K., 2005. Intensity and coherence of motifs in weighted complex networks. Phys Rev E Stat Nonlin Soft Matter Phys. 71(6 Pt 2):065103.

Oh, E.S., Savonenko, A.V., King, J.F., Fangmark Tucker, S.M., Rudow, G.L., Xu, G., Borchelt, D.R., Troncoso, J.C., 2009. Amyloid precursor protein increases cortical neuron size in transgenic mice. Neurobiol Aging 30, 1238-1244.

Oh, H., Habeck, C., Madison, C., Jagust, W., 2014. Covarying alterations in Aβ deposition, glucose metabolism, and gray matter volume in cognitively normal elderly. Hum Brain Mapp. 35, 297-308.

Petrie, E.C., Cross, D.J., Galasko, D., Schellenberg, G.D., Raskind, M.A., Peskind, E.R., Minoshima, S., 2009. Preclinical evidence of Alzheimer changes: convergent cerebrospinal fluid biomarker and fluorodeoxyglucose positron emission tomography findings. Arch Neurol. 66, 632-637.

Pettigrew, C., Soldan, A., Moghekar, A., Wang, M.C., Gross, A.L., O'Brien, R., Albert, M., 2015. Relationship between cerebrospinal fluid biomarkers of Alzheimer's disease and cognition in cognitively normal older adults. Neuropsychologia 78, 63-72.

Reiman, E.M., Langbaum, J.B., Tariot, P.N., 2010. Alzheimer's prevention initiative: a proposal to evaluate presymptomatic treatments as quickly as possible. Biomark Med. 4, 3-14.

Roe, C., Fagan, A., Grant, E., Hassenstab, J., Moulder, K., Dreyfus, D., Morris, J., 2013. Amyloid imaging and CSF biomarkers in predicting cognitive impairment up to 7.5 years later. Neurology 80, 1784-1791.

Romero-Garcia, R., Atienza, M., Clemmensen, L.H., Cantero, J.L., 2012. Effects of network resolution on topological properties of human neocortex. Neuroimage 59, 3522-3532.

Romero-Garcia, R., Atienza, M., Cantero, J.L., 2014. Predictors of coupling between structural and functional cortical networks in normal aging. Hum Brain Mapp. 35, 2724-2740.

Romero-Garcia, R., Atienza, M., Cantero, J.L., 2016. Different scales of cortical organization are selectively targeted in the progression to Alzheimer's disease. Int J Neural Syst. 26, 1650003.

Rosas, H.D., Liu, A.K., Hersch, S., Glessner, M., Ferrant,e R.J., Salat, D.H., van der Kouwe, A., Jenkins, B.G., Dale, A.M., Fischl, B., 2002. Regional and progressive thinning of the cortical ribbon in Huntington's disease. Neurology 58, 695-701.

Rosenberg, P.B., Wong, D.F., Edell, S.L., Ross, J.S., Joshi, A.D., Brašić, J.R., Zhou, Y., Raymont, V., Kumar, A., Ravert, H.T., Dannals, R.F., Pontecorvo, M.J., Skovronsky, D.M., Lyketsos, C.G., 2013. Cognition and amyloid load in Alzheimer disease imaged with florbetapir F 18(AV-45) positron emission tomography. Am J Geriatr Psychiatry 21, 272-278.

Rubinov, M., Sporns, O., 2010. Complex network measures of brain connectivity: uses and interpretations. Neuroimage 52, 1059-1069.

Sala-Llonch, R., Lladó, A., Fortea, J., Bosch, B., Antonell, A., Balasa, M., Bargalló, N., Bartrés-Faz, D., Molinuevo, J.L., Sánchez-Valle, R., 2015. Evolving brain structural changes in PSEN1 mutation carriers. Neurobiol Aging 36, 1261-1270.

Salat, D.H., Buckner, R.L., Snyder, A.Z., Greve, D.N., Desikan, R.S., Busa, E., Morris, J.C., Dale, A.M., Fischl, B., 2004. Thinning of the cerebral cortex in aging. Cereb Cortex 14, 721-730.

Scheperjans, F., Eickhoff, S.B., Hömke, H., Mohlberg, K., Hermann, K., Amunts, K., Zilles, K., 2008. Probabilistic maps, morphometry, and variability of citoarchitectonic areas in the human superior parietal cortex. Cereb. Cortex 18, 2141-2157.

Schneider, R.C., Crosby, E.C., Farhat, S.M., 1965. Extratemporal lesions triggering the temporal-lobe syndrome. J Neurosurg. 22, 246-263.

Sheline, Y.I., Raichle, M.E., Snyder, A.Z., Morris, J.C., Head, D., Wang, S., Mintun, M.A., 2010. Amyloid plaques disrupt resting state default mode network connectivity in cognitively normal elderly. Biol Psychiatry 67, 584-587.

Singh, V., Chertkow, H., Lerch, J.P., Evans, A.C., Dorr, A.E., Kabani, N.J., 2006. Spatial patterns of cortical thinning in mild cognitive impairment and Alzheimer's disease. Brain 129, 2885-2893.

Sorg, C., Riedl, V., Mühlau, M., Calhoun, V.D., Eichele, T., Läer, L., Drzezga, A., Förstl, H., Kurz, A., Zimmer, C., Wohlschläger, A.M., 2007. Selective changes of resting-state networks in individuals at risk for Alzheimer's disease. Proc Natl Acad Sci USA 104, 18760-18765.

Spreng, R.N., Turner, G.R., 2013. Structural covariance of the default network in healthy and pathological aging. J Neurosci. 33, 15226-15234.

Stam, C.J., Jones, B.F., Nolte, G., Breakspear, M., Scheltens, P., 2007. Small-world networks and functional connectivity in Alzheimer's disease. Cereb Cortex 17, 92-99.

Stomrud, E., Forsberg, A., Hägerström, D., Ryding, E., Blennow, K., Zetterberg, H., Minthon, L., Hansson, O., Londos, E., 2012. CSF biomarkers correlate with cerebral blood flow on SPECT in healthy elderly. Dement Geriatr Cogn Disord. 33, 156-163.

Storandt, M., Mintun, M.A., Head, D., Morris, J.C., 2009. Cognitive decline and brain volume loss as signatures of cerebral amyloid-beta peptide deposition

identified with Pittsburgh compound B: cognitive decline associated with Abeta deposition. Arch Neurol. 66, 1476-1481.

Strozyk, D., Blennow, K., White, L.R., Launer, L.J., 2003. CSF Abeta 42 levels correlate with amyloid-neuropathology in a population-based autopsy study. Neurology 60, 652-656.

Tapiola, T., Alafuzoff, I., Herukka, S.K., Parkkinen, L., Hartikainen, P., Soininen, H., Pirttilä, T., 2009. Cerebrospinal fluid beta-amyloid 42 and tau proteins as biomarkers of Alzheimer-type pathologic changes in the brain. Arch Neurol. 66, 382-389.

Thompson, P.M., Hayashi, K.M., de Zubicaray, G., Janke, A.L., Rose, S.E., Semple, J., Herman, D., Hong, M.S., Dittmer, S.S., Doddrell, D.M., Toga, A.W., 2003. Dynamics of gray matter loss in Alzheimer's disease. J Neurosci. 23, 994-1005.

Tijms, B.M., Möller, C., Vrenken, H., Wink, A.M., de Haan, W., van der Flier, W.M., Stam, C.J., Scheltens, P., Barkhof, F., 2013. Single-subject grey matter graphs in Alzheimer's disease. PLoS One 8(3):e58921.

Tijms, B.M., Kate, M.T., Wink, A.M., Visser, P.J., Ecay, M., Clerigue, M., Estanga, A., Garcia Sebastian, M., Izagirre, A., Villanua, J., Martinez Lage, P., van der Flier, W.M., Scheltens, P., Sanz Arigita, E., Barkhof, F., 2016. Gray matter network disruptions and amyloid beta in cognitively normal adults. Neurobiol Aging 37, 154-160.

Toledo, J.B., Weiner, M.W., Wolk, D.A., Da, X., Chen, K., Arnold, S.E., Jagust, W., Jack, C., Reiman, E.M., Davatzikos, C., Shaw, L.M., Trojanowski, J.Q.; Alzheimer’s Disease Neuroimaging Initiative., 2014. Neuronal injury biomarkers and prognosis in ADNI subjects with normal cognition. Acta Neuropathol Commun. 2:26.

Tosun, D., Schuff, N., Truran-Sacrey, D., Shaw, L.M., Trojanowski, J.Q., Aisen, P., Peterson, R., Weiner, M.W.; Alzheimer's Disease Neuroimaging Initiative., 2010. Relations between brain tissue loss, CSF biomarkers, and the ApoE genetic profile: a longitudinal MRI study. Neurobiol Aging 31, 1340-1354.

Travers, J., Milgram, S., 1969. An experimental study of the small world problem. Sociometry 32, 425-443.

Trojanowski, J.Q., Schuck, T., Schmidt, M.L., Lee, V.M., 1989. Distribution of tau proteins in the normal human central and peripheral nervous system. J Histochem Cytochem. 37, 209-215.

Wang, L., Benzinger, T.L., Hassenstab, J., Blazey, T., Owen, C., Liu, J., Fagan, A.M., Morris, J.C., Ances, B.M., 2015. Spatially distinct atrophy is linked to β-amyloid and tau in preclinical Alzheimer disease. Neurology 84, 1254-1260.

Wu, K., Taki, Y., Sato, K., Kinomura, S., Goto, R., Okada, K., Kawashima, R., He, Y., Evans, A.C., Fukuda, H., 2012. Age-related changes in topological organization of structural brain networks in healthy individuals. Hum Brain Mapp. 33, 552-568.

Yao, Z., Zhang, Y., Lin, L., Zhou, Y., Xu, C., Jiang, T; Alzheimer's Disease Neuroimaging Initiative., 2010. Abnormal cortical networks in mild cognitive impairment and Alzheimer's disease. PLoS Comput Biol. 6(11):e1001006.

Zhang, Y., Schuff, N., Jahng, G.H., Bayne, W., Mori, S., Schad, L., Mueller, S., Du, A.T., Kramer, J.H., Yaffe, K., Chui, H., Jagust, W.J., Miller, B.L., Weiner, M.W., 2007. Diffusion tensor imaging of cingulum fibers in mild cognitive impairment and Alzheimer disease. Neurology 68, 13-19.

Table 1. Demographic, CSF markers and cognitive profile.

	Controls	$A\beta_{1-42}^{+}$	p-tau^{+}
$A\beta_{1-42}$ (pg/mL)	855.3 ± 75.9	471.2 ± 74.2**	884.7 ± 236.8
p-tau (pg/mL)	32.6 ± 4.9	29.4 ± 10.1	79.3 ± 19.1**
Age	59 ± 6.1	61.2 ± 7.8	63.3 ± 8.8*
Gender (m/f)	4/16	5/14	4/14
Education, years	13.3 ± 3.7	13 ± 4.6	12.9 ± 4.5
ApoE ε4 (yes/no)	2/18	10/9	4/14
MMSE	29.4 ± 0.7	28.8 ± 1	28.7 ± 1.3
Boston naming test	53.5 ± 5.1	54.4 ± 3.4	54.7 ± 3.1
Clock test	9.8 ± 0.3	9.6 ± 0.4	9.8 ± 0.4
Word list	5.3 ± 0.8	5.2 ± 1	5.1 ± 0.8
Rey figure	33.6 ± 1.9	33.1 ± 1.6	32.6 ± 1.8
VOSP	9.2 ± 1.5	9.1 ± 0.8	9.1 ± 1.7

Results are expressed as mean ± standard deviation. m/f: male/female; MMSE: Mini Mental State Examination; VOSP: Visual Object and Space Perception Battery. *p=0.001; **$p<10^{-8}$

Table 2. Group differences in cortical thickness

Cortical region (BA)	CS (mm^2)	Mean ± SD thickness (mm)		Change (%)	*P*
$A\beta_{1\text{-}42}^{+}$ > Controls		**Controls**	**$A\beta_{1\text{-}42}^{+}$**		
Left middle temporal	1512	2.37 ± 0.15	2.42 ± 0.15	3	10^{-4}
Controls > p-tau^{+}		**Controls**	**p-tau^{+}**		
Left superior parietal	171	2.43 ± 0.2	2.01 ± 0.21	17	10^{-5}
Left medial orbitofrontal	406	2.47 ± 0.22	2.1 ± 0.24	15	10^{-4}
Right precuneus	328	2.44 ± 0.23	2.12 ± 0.27	14	10^{-3}

SD: standard deviation; mm: millimeters; CS: cluster size; *P*: corrected *p*-value using the hierarchical statistical model (Bernal-Rusiel et al., 2010).

Table 3. Group differences in cerebral WM volume

WM tract	CS (mm^3)	x	y	z	P
Controls > $A\beta_{1\text{-}42}^{+}$					
Left cingulum parahippocampal	1767	-22	-53	1	10^{-4}
Right subgenual cingulum	451	12	40	31	0.004
Controls > p-tau^{+}					
Left cingulum parahippocampal	1602	-17	-42	-1	10^{-5}
Left uncinate fasciculus	574	-33	-3	-18	0.003

WM: white matter; CS: cluster size; mm: millimeters; *P*: corrected *p*-value using the family wise error rate ($p<0.05$). Coordinates (x-y-z) are in the MNI anatomical space, and correspond to the voxel of maximum significance within the cluster. Location of affected WM regions were obtained with the JHU white-matter tractography atlas (Hua et al., 2008).

Table 4. Group differences in the inward/outward connectivity metric for each cortical lobe.

Cortical lobe	Controls	$A\beta_{1\text{-}42}^{+}$	p-tau^{+}
Left frontal	1.34	1.47	1.04
Left parietal	1.26	1.46	0.76
Left temporal	1.64	1.79	1.66
Left occipital	1.58	2.33	3.32
Left cingulate	2.17*	6.74*	5.04
Right frontal	2.15	2.32	1.94
Right parietal	1.65	1.97	2.14
Right temporal	1.84*	3.73*	1.87
Right occipital	3.51	6.15	4.11
Right cingulate	3.07	3.29	1.33

Higher values in this metric reflect more lobular segregation. The asterisk (*) indicates that group differences ($A\beta_{1\text{-}42}^{+}$ > controls) was statistically significant ($p < 0.05$).

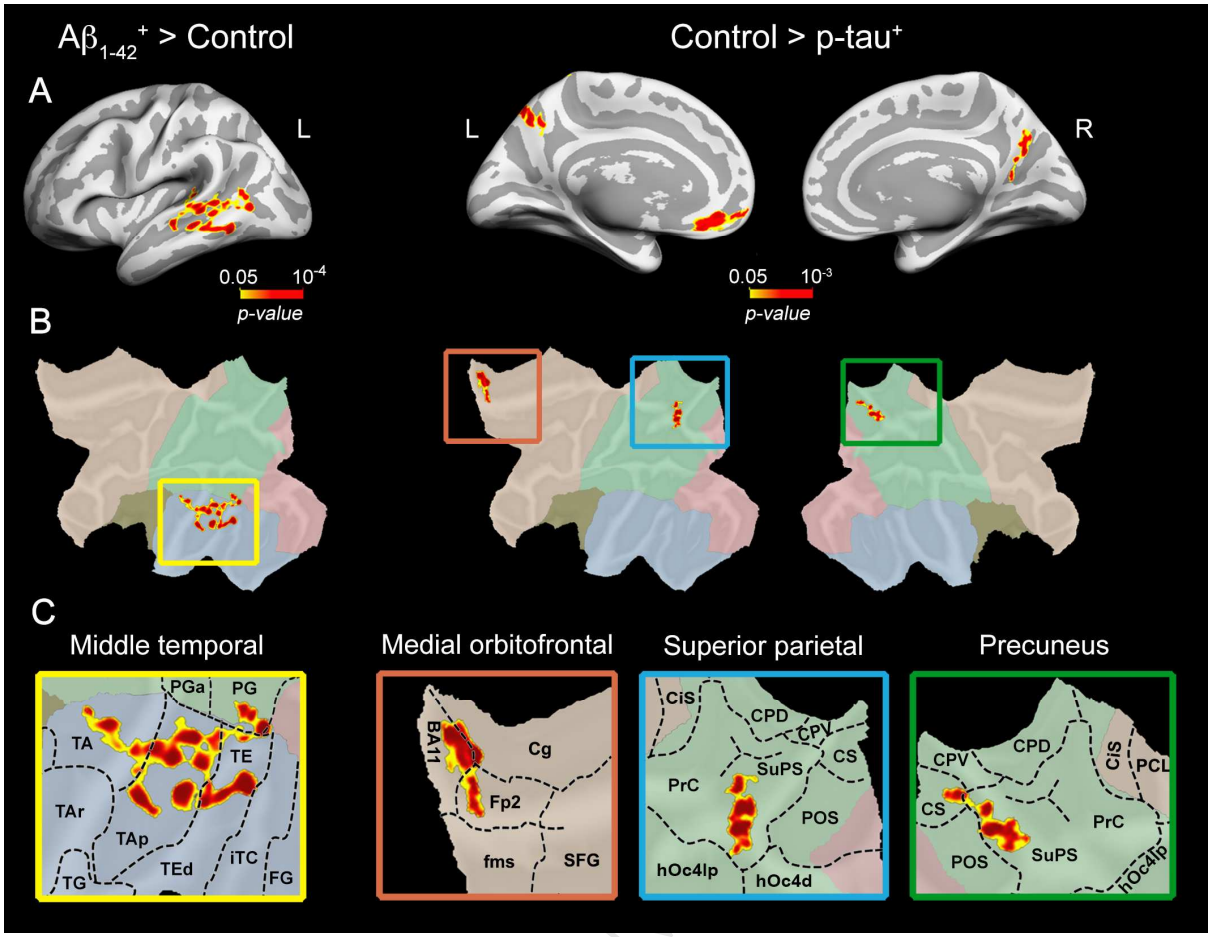

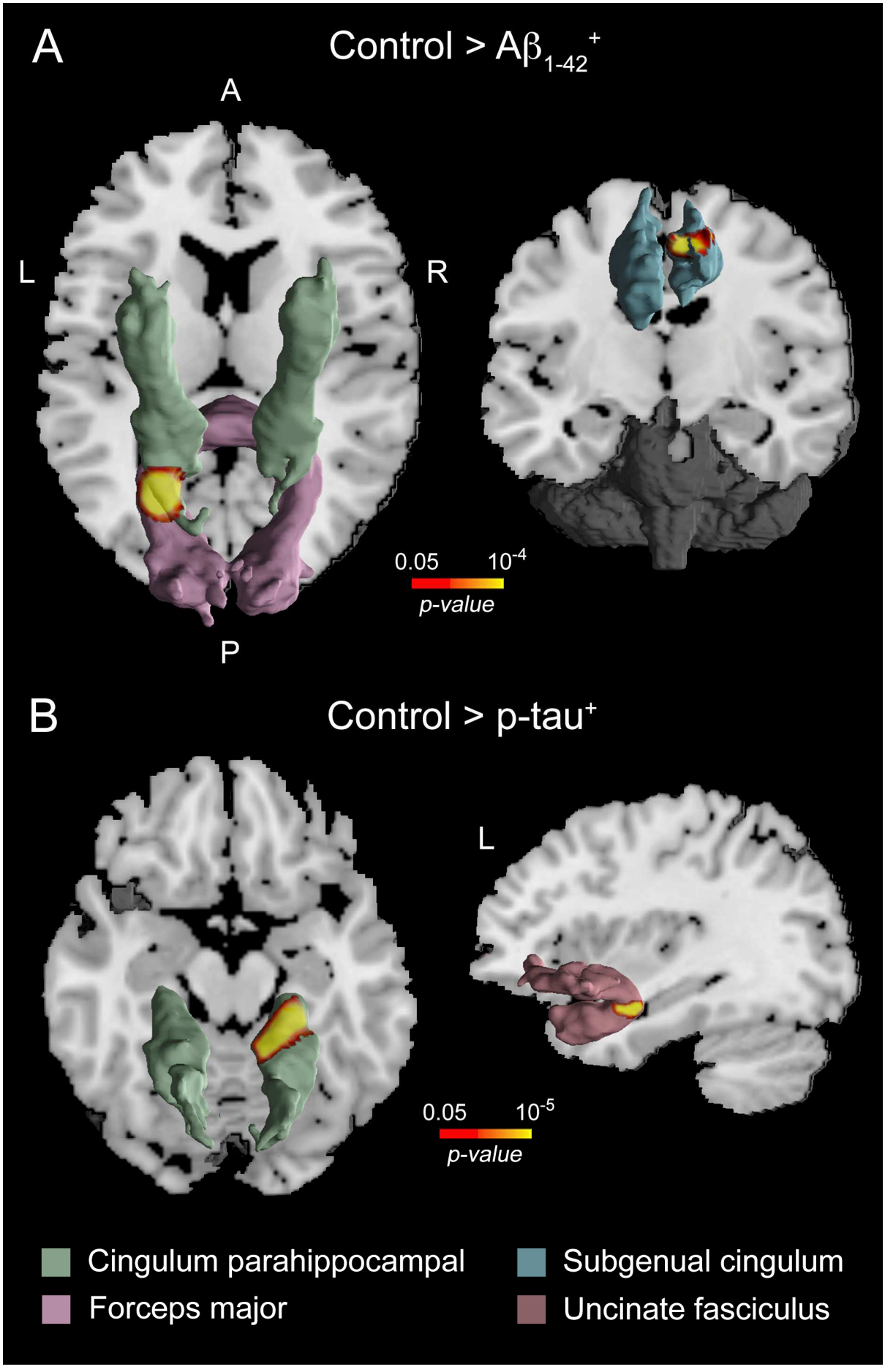
A
Control > Aβ1-42+
A
L
R
P
0.05
10-4
p-value
B
Control > p-tau+
L
0.05
10-5
p-value
Cingulum parahippocampal
Forceps major
Subgenual cingulum
Uncinate fasciculus

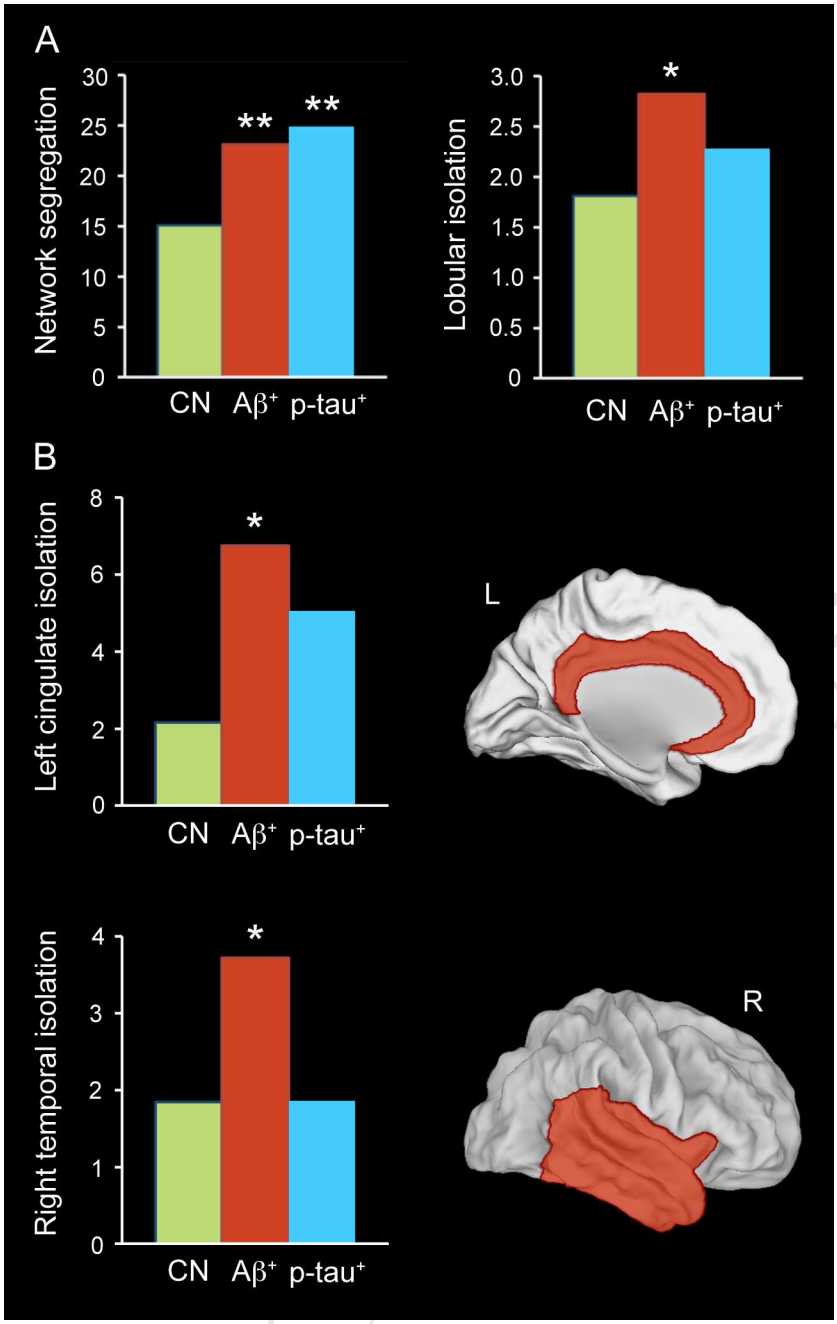

Highlights

- CSF $A\beta_{1\text{-}42}^{+}$ subjects show thickening of the middle temporal cortex.
- CSF p-tau^{+} subjects show thinning of the fronto-parietal cortices.
- Abnormal CSF levels of $A\beta_{1\text{-}42}$ and p-tau are associated with WM atrophies.
- Abnormal CSF levels of $A\beta_{1\text{-}42}$ and p-tau are associated with cortical segregation.